

NJC

Accepted Manuscript



This is an *Accepted Manuscript*, which has been through the Royal Society of Chemistry peer review process and has been accepted for publication.

Accepted Manuscripts are published online shortly after acceptance, before technical editing, formatting and proof reading. Using this free service, authors can make their results available to the community, in citable form, before we publish the edited article. We will replace this *Accepted Manuscript* with the edited and formatted *Advance Article* as soon as it is available.

You can find more information about *Accepted Manuscripts* in the [Information for Authors](#).

Please note that technical editing may introduce minor changes to the text and/or graphics, which may alter content. The journal's standard [Terms & Conditions](#) and the [Ethical guidelines](#) still apply. In no event shall the Royal Society of Chemistry be held responsible for any errors or omissions in this *Accepted Manuscript* or any consequences arising from the use of any information it contains.

A biopolymer gel decorated cobalt molybdate nanowafer: Effective graft polymer cross-linked with an organic acid for better energy storage

Ramya Ramkumar and Manickam Minakshi Sundaram*

School of Engineering and Information Technology, Murdoch University, WA 6150, Australia

Abstract

Nanoflake-like α -CoMoO₄ was prepared with the aid of cationic surfactant, cetyltrimethylammonium bromide (CTAB), as electrode material for supercapacitor by scalable solution combustion synthesis (SCS). The specific capacitance of the fabricated hybrid device (CoMoO₄/CTAB vs. activated carbon (AC)) exhibits marginal increase in specific capacitance of 39 F/g to that of the as-prepared (parent) CoMoO₄ with 24 F/g. To achieve better energy storage, modification was done on CoMoO₄ by grafting chitosan in the presence of a weak, acetic acid (AA) or citric acid (CA) as a crosslinking agent. A biopolymer, chitosan is cross-linked using CA as a cross-linker while in the case of acetic acid, grafting of chitosan/AA does not occur. The improved properties of chemical and polymer modified CoMoO₄ were evaluated using physical and electrochemical methods and compared with as-prepared (parent) compound. The polymer modified composite exhibited the maximum specific capacitance of 71 F/g at 2 mA cm⁻² with capacity retention of 81% after 2000 cycles, about twofold higher than that of chemical modified electrode. Influence of surfactant and chitosan concentration on the specific capacitance is also established. A solid state capacitor was fabricated using CoMoO₄ vs. AC, with chitosan as the gel separator. High resolution transmission electron microscopy (HR-TEM) and field emission scanning electron microscopy (FE-SEM) images support the cross-linking strategy and nanowafer like morphology with honeycomb arrangement.

Keywords: Cobalt molybdate; chitosan; activated carbon; surfactant; polymer.

*E: m.minakshi-sundaram@murdoch.edu.au

1. Introduction

As the concerns grow over fossil fuel usage and depletion of available resources, renewable energy plays a niche in the market.¹ Renewable energy is readily available but not affordable due to the technological barriers found in the existing energy storage systems.² The essential requirements of an energy storage device for storing renewable energy are low cost, long cycle life and environmental friendly materials.³ Electrochemical energy storage systems comprising batteries (with high energy density) coupled with capacitors (high cycling performance and power density) offer many benefits and merits compared with conventional forms of energy storage. Supercapacitors are considered as attractive power sources due to its rapid charging – discharging rates and make it vital for quick power delivery.⁴ Depending on the storage mechanism, supercapacitors have been grouped into two different types (a) electric double-layer capacitors based on non-Faradaic type and (b) pseudocapacitors that develop reversible redox reactions (Faradaic) for charge storage. Hybrid capacitors also termed as “asymmetric” combines the features of supercapacitors and batteries.⁵ The specific energy of the hybrid device can be enhanced by tailoring the suitable materials.

The most commonly investigated classes of materials are transition metal oxides/hydroxides⁶⁻⁸, molybdates⁹⁻¹⁰, phosphates¹¹⁻¹², and conducting polymers¹³⁻¹⁴ etc., which exhibit reversible redox charge transfer. The available capacitance from the conducting polymers and transition metal phosphates is high but the conducting polymers have poor cycling stability whereas the metal phosphates have poor conductivity.¹¹⁻¹⁴ On the other hand, transition metal oxides have been widely used as potential electrode materials in supercapacitors but the drawback is being relatively very expensive. Among the different metal oxides, notably ruthenium oxide (RuO_2) delivers high capacitance but its use is limited because of high cost.¹⁵ Hence, recently researchers have focussed on other base transition metal oxides as alternatives. In-expensive transition metal oxides such as NiO , MnO_2 , Cr_2O_3 ,

and Co_3O_4 have been reported as potential electrode materials for supercapacitors.¹⁶⁻¹⁸ Manganese dioxide (MnO_2) is believed to be a promising material because of their abundant resources, low cost, environmental friendly, wide electrochemical window, rich redox chemistry and high theoretical specific capacitance. To increase the capacitance of MnO_2 , various additives such as carbon nanotubes, graphene and conducting polymers have been examined and reported.¹⁹⁻²⁰ Further to this, range of synthetic strategies have also been employed that led to the formation of 1D and 2D MnO_2 particles with nanotube, nanoplate, nanosphere and nanowire morphologies.²¹ This enhanced the activity of the MnO_2 electrode material, however, it suffered from the limited cycling stability due to formation of Jahn-Teller distortion. The Cr_2O_3 , NiO and Co_3O_4 counterparts have also been severely plagued due to narrow operating voltage, coulombic efficiency, and poor cyclability.¹⁸

Alternatively, molybdates are attractive compounds for hybrid capacitor applications because of their structural, magnetic, catalytic and electrochemical properties.¹⁰ Metal molybdates have been considered as semiconducting materials which is used in catalysis, photoluminescence sensors, magnetic and energy storage applications. Not only molybdates but also the metal cations such as Co, Ni or Fe in the framework possess high electrochemical activity which enhances the performance of supercapacitors. Reports on molybdates, in particular, CoMoO_4 and its suitability for energy storage applications are limited.^{10, 22-23} The Ni based molybdates owes high redox couple and Co substitution for Ni sites resulting as solid-solution compound i.e. $\text{Ni}_x\text{Co}_{1-x}\text{MoO}_4$ ²⁴ has been well reported and found suitable for energy storage applications.²⁵ Likewise, the multi-metal composites, $\text{MnMoO}_4/\text{CoMoO}_4$ having heterostructured nanowires have been reported for supercapacitor applications.¹⁰ Cobalt molybdate (CoMoO_4) is particularly attractive because of its one-step synthesis, low production cost, non-toxic with high redox potential.^{23,26} The reported supercapacitive

properties for this material are marginal and neither chemical nor polymer approaches are yet well established.

The significance and novelty of the current work lies in decorating the material using two different strategies i.e. chemical and polymer modified CoMoO₄ composites in order to enhance the specific capacitance of CoMoO₄ reported in the literature.^{10,22-26} The chemical modification was carried out with a cationic surfactant cetyltrimethylammonium bromide (CTAB). The behaviour of CTAB that facilitates the surface morphology and its influence in supercapacitive properties has not been well explored for CoMoO₄. Considering the enormous industrial importance of surfactants^{7,27}, the current work was undertaken with the objective of studying its behaviour in electrochemical performance. Interestingly, the chemically modified electrode, surfactant assisted in preventing the particle aggregation and also led to carbon deposits on the parent material. The porous CoMoO₄/CTAB composites having the edges of nanoflakes are smaller in size than that of CoMoO₄ reported in one of our earlier publications.²⁴ The surfactant leaves a carbon residue on the surface of CoMoO₄ and increases the capacitance, however it is marginal. Hence, an alternative biopolymer approach was also undertaken in the present work.

Towards the polymer approach, the biopolymer used in this study is chitosan. Chitosan is a polysaccharide containing two repeating units made of GlucNAc(N-acetyl glucosamine) and GlucN(glucosamine).²⁸ The chitosan can be obtained by the deacetylation of chitin found in the shells of crustaceans. Chitosan possess excellent properties, such as inexpensive, biocompatible, and biodegradable. Chitosan is able to sorb metal anions such as molybdates soluble in weak organic acids like acetic, citric, ascorbic, glutamic, lactic, maleic, malic and succinic.²⁹ In this study, we were interested to use chitosan in the presence of weak acetic acid (AA) or citric acid (CA) as cross-linkers and to determine its influence in the redox activity and compared to the as-prepared CoMoO₄. Chitosan dissolved in weak acid

can be cross-linked using various agents including diamines, polyamines, diols, polyols, and polyoxides.³⁰ However, the citric acid forms an ionic complex with chitosan because of its multivalent character in nature.³¹

The use of chitosan as biopolymer increased the specific capacitance significantly by the affinity with molybdate moiety and its extent of performance depends on the cross-linker employed. The primary advantage of cross-linking is that it improves the surface functionality of the modified electrode. A solid state device was also fabricated using the biopolymer gel as the electrolyte and the preliminary results have been reported. Although there are a few reports on synthetic gel based separators³², redox mediated gel electrolytes³³ and gel based electrode binders³⁴ for electrochemical double layers capacitors (EDLC) but to the best of our knowledge, chitosan cross-linked with organic acids such as acetic (or) citric hasn't been reported for metal molybdates. The graft polymerization of organic acids with chitosan is a new approach to obtain relatively uniform and porous structure of host polymer for energy storage applications. While, the conventional chitosan-glutaraldehyde reaction reported in one of our earlier publications²⁴ resulted in less uniform structure due to faster gelation process. This suggests that the formation of the salt is dependent on the nature of the cross-linker. A contribution to enhance the energy storage properties, and the mechanism of the polymeric structure formed is proposed in this work. The fabrication of solid state devices (activated carbon *vs.* CoMoO₄) using biopolymer electrolyte is a novel approach and our initial results showed an ideal capacitive behaviour. Overall, the current study might find application in the fundamental chemistry of surfactants and polymers, as well as in the energy storage system and advance the performance of the CoMoO₄ material reported by us earlier.²³⁻²⁴ A detailed physical and electrochemical characterization has been carried on the as-prepared (parent), chemical and polymer modified compounds and discussed.

2. Experimental

2.1 Materials

Cobalt molybdate was synthesized by a template assisted solution combustion technique²³, in which a high purity $\text{Co}(\text{NO}_3)_2 \cdot 6\text{H}_2\text{O}$ (6.648 g), $(\text{NH}_4)_6\text{Mo}_7\text{O}_{24} \cdot 4\text{H}_2\text{O}$ (4.033 g), and $\text{CO}(\text{NH}_2)_2$ (1.699 g) as a fuel in 20 mL of deionized water were used. All the chemical reagents used were analytical reagent (AR) grade obtained from Sigma – Aldrich and used as received without further purification. The oxidant to fuel ratio was maintained at 1:1. Ammonia solution was added dropwise to adjust the pH of the solution to 8. The precursors were just heated at 300 °C for an hour to obtain the final product CoMoO_4 and no further calcination was done to the obtained product. The chemical modified material was also synthesized in an identical way except the addition of cationic surfactant, cetyltrimethylammonium bromide (CTAB). The solution of CTAB with a concentration of 0.25 mg/mL was added to the molybdate precursors in 20 mL of deionized water and followed a very similar procedure of synthesis. For polymer modified CoMoO_4 , chitosan of low molecular weight (50 – 190 kDa) purchased from Sigma – Aldrich with a deacetylation degree of 75 – 85 % was dissolved in either acetic acid (AA) or citric acid (CA) and stirred with a magnetic stirrer until complete dissolution of chitosan to a clear solution. The resulting chitosan solution was poured into a petri dish and, after the solvent has evaporated, the gel was neutralised with 0.20 mol dm³ solution of NaOH so that the pH was raised to a value between 6.0 and 7.0. To the resultant gel, having the best concentration, as-prepared CoMoO_4 powder was added and thoroughly stirred for 5 min in order to be homogenised. At near neutral pH, the cations Co^{2+} are found as free ions in aqueous solutions and can be adsorbed onto biopolymer chitosan by chelation according to the following equation (1)



An insight into the role of CTAB surfactant and AA or CA cross-linker for the grafting of chitosan onto CoMoO₄ and its adsorption capacity of Co²⁺ metal cations are given in detail in Figs. S1 – S4 (ESI[§]). The schematic representation of grafted CoMoO₄/chitosan composite is shown in Fig. S5 (ESI[§]).

2.2 Characterization

The morphology and crystal structure of the as-prepared and modified CoMoO₄ were investigated using X-ray Diffractometer, high magnification Zeiss Neon 40EsB focussed ion beam-scanning electron microscope (FIB-SEM), transmission electron microscopy (TEM) associated with energy dispersive X-ray detector (EDS) using a JEOL 2010F TEM operated at 200 kV. TEM specimens were prepared by grinding a small fragment of CoMoO₄ powder material under methanol and dispersing on a holey carbon support film. Specimens were examined at liquid nitrogen temperature in a cooling stage, to reduce beam damage and contamination effects. Phase identification was carried out by powder X-ray diffraction (XRD) using Siemens D500 X-ray diffractometer 5635 with Cu-K α source at a scan speed of 1° /min. The voltage and current were 40 kV and current 28 mA, respectively. X-ray photoelectron spectroscopy (XPS) using monochromatic Al K α (1486.6 eV) radiation was used to analyse the chemical binding energy of the samples. Carbon (1s) was used as a reference for all samples. Attenuated total reflectance-Fourier transform infrared (ATR-FTIR) studies were carried out with a Bruker IFS 125/HR spectrometer. The nitrogen adsorption-desorption isotherms were measured at 77 K using Micromeritics Tristar II surface area and porosity analyser. Before analysing the samples were degassed at 80 °C overnight. The surface area was calculated by the Brunauer-Emmett-Tellet (BET) method. Rutherford back scattering analysis (RBS) is used in conjunction with proton induced X-ray emission (PIXE) to determine the concentrations of elements such as Co, Mo and C. The RBS and PIXE measurements were made simultaneously on an ion beam accelerator using a

3 MeV He⁺ proton beam at ANSTO facilities. The electrochemical measurements were carried out using an electrochemical working station (BioLogic SP-150 instrument) with two electrode cells at room temperature. The electrolyte was 2 M NaOH aqueous solution.

2.3 Device Fabrication and Measurements

For electrochemical measurements, graphite sheets were polished with emery paper then washed with running distilled water and ultrasonicated for 15 min until it is free of any suspended particles. Finally, the sheet is dried at 60° C for 15 min and employed as the working electrode. The electrode material was either CoMoO₄ or Activated carbon (AC) (85 wt.%), carbon black (10 wt.%) and polyvinylidene fluoride (5 wt.%) were suspended 0.4mL of N-methyl-2-pyrrolidinone (NMP) to form a slurry. An aliquot (10 μL) of the slurry was coated on the graphite sheet (area of coating: 1 cm²) to give a total mass of the electrode material of 2 mg. A solution of 2M NaOH was used as the electrolyte. The asymmetric cell was fabricated using activated carbon (AC) as negative electrode and CoMoO₄ as the positive electrode on the graphite sheet. The cut-off charge and discharge voltages were 1.5 and 0.2 V. Electrochemical impedance spectroscopy was carried out with amplitude of 10 mV over a frequency range 10 mHz to 200 kHz at open circuit potential. For a solid state device, chitosan dissolved in acetic acid and cross-linked with gluteraldehyde was used as the separator. The optimal mass ratio between cobalt molybdate and activated carbon (as-received from Sigma Aldrich with a surface area of 1800 m² g⁻¹) was determined to be 1.6 for the fabricated hybrid capacitor. The mass balance was calculated using the following equation (2)

$$m^+ / m^- = (C_- * \Delta E_-) / (C_+ * \Delta E_+) \quad (2)$$

where C is the specific capacitance; ΔE is the potential range for the charge / discharge processes. The mass of the positive and negative electrode material was 2.0 and 3.2 mg,

respectively. The calculated capacitances from the cyclic voltammetry and charge discharge studies at 5 mV s^{-1} and 1 mA cm^{-2} (in Table 1 and 2) are the data presented with replicates of five samples and in an average of several cycles each with a standard deviation with a narrow range of only $3.66 (\pm 2\%)$.

3. Results and Discussion

3.1. Structural studies of CoMoO_4

The structural characterization of the CoMoO_4 composites has been performed by the X-ray diffraction (XRD) analysis. The diffraction patterns of the chemical and polymer modified are compared with the as-prepared (parent) CoMoO_4 in Figure 1.

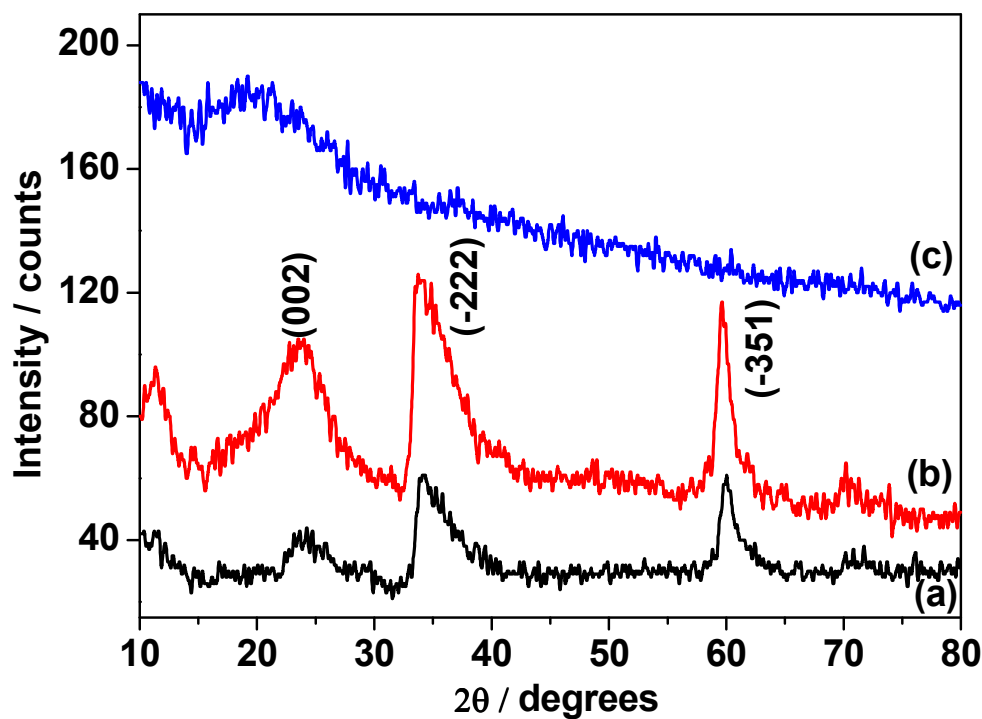
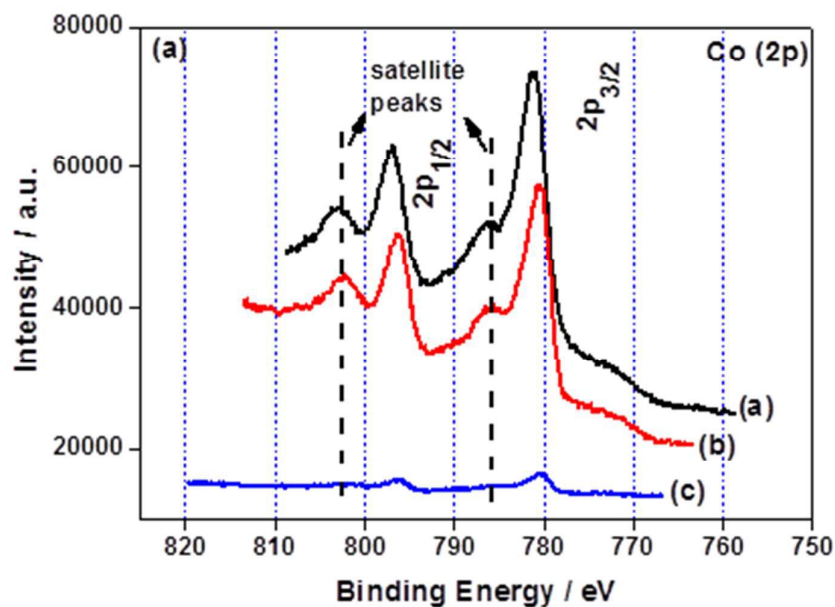


Figure 1 X-ray diffraction (XRD) patterns of (a) as-prepared (b) chemical modified and (c) polymer modified CoMoO_4 .

The diffraction pattern of the parent and chemical modified CoMoO_4 (in the absence and presence of CTAB) in Fig 1a and b, exhibits similar diffraction peaks suggesting that the CTAB composites have not acquired additional crystalline structure. The obtained peaks are in well agreement with the CoMoO_4 (JCPDS file 21-0868), however, the as-prepared materials synthesized at 300 °C without any further calcination possessing a broad and diffused pattern reveals an amorphous nature. For polymer modified sample (Fig 1c), no diffraction peaks are observed but instead it has a broad hump. This may be due to the degree of polymerization and the surface functionality that affects the crystallinity of the CoMoO_4 . The formation of strong covalent interactions from the grafting of polymer chains between chitosan and citric acid improved the compatibility of the polymer but reduced the crystallinity of cobalt molybdate.³⁵⁻³⁶ The characteristics of the surface elements were investigated by X-ray photoelectron spectroscopy (XPS) technique. Figure 2 shows the high resolution XPS spectra of Co (2p), C (1s) and O (1s) for the CoMoO_4 samples.



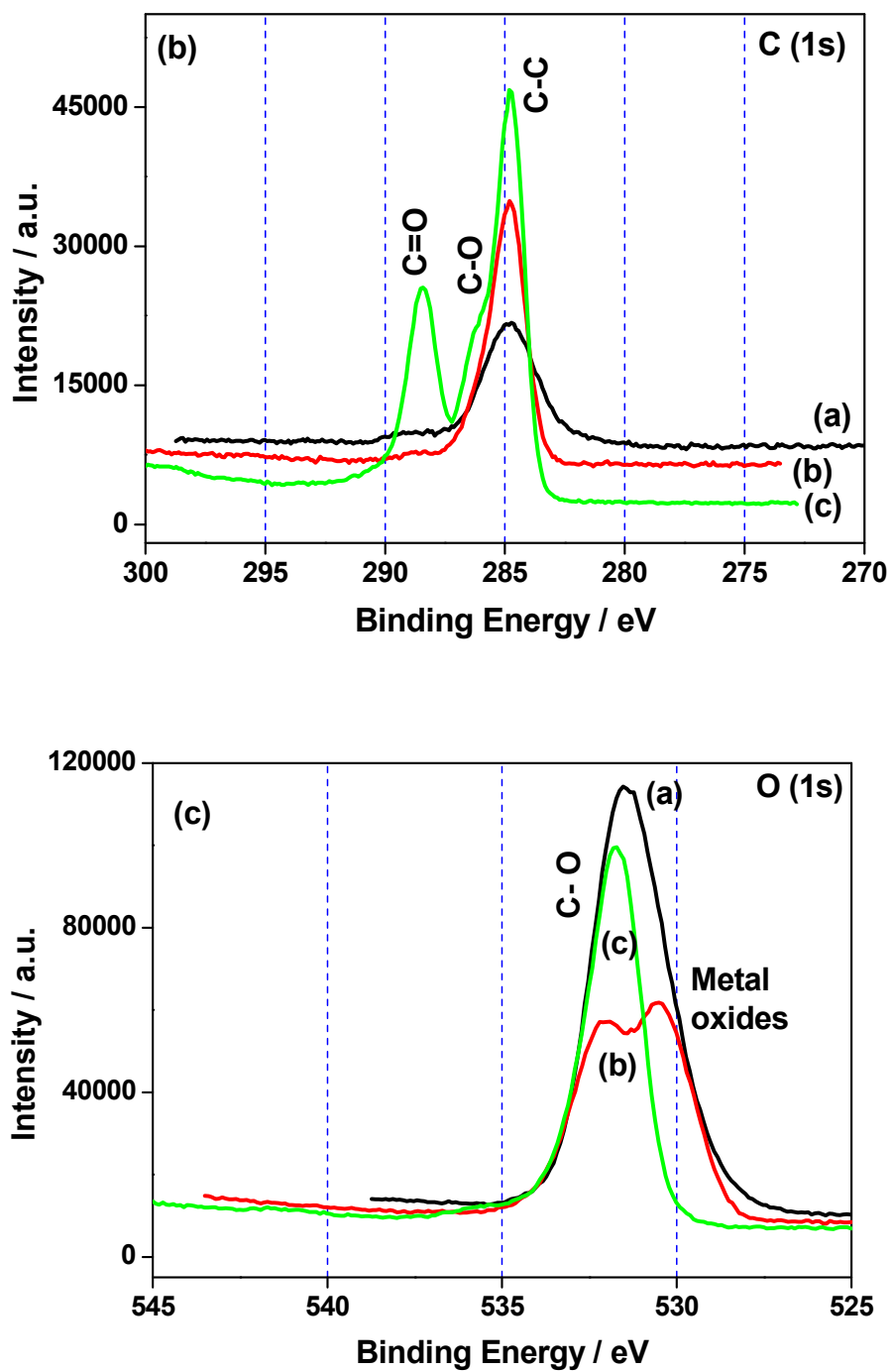


Figure 2 XPS spectra of Co (2p), C (1s) and O (1s) for the (a) as-prepared (b) chemical modified and (c) polymer modified CoMoO₄.

Figure 2a shows the XPS spectra of Co (2p). The Co2p_{1/2} and 2p_{3/2} split spin orbit components have been observed at 797 and 781 eV respectively, for both parent and chemically modified CoMoO₄ samples with fairly similar intensities. A satellite peak for each 2p_{3/2} and 2p_{1/2} components is also observed at 786 and 802 eV respectively. The observed peaks are quite similar to those reported for this compound in the literature.³⁷ As can be seen in Fig. 2a, a chemical shift of 0.5 eV towards lower binding energy is observed for chemical modified sample. This chemical shift reflects the chemical affinity between cationic surfactant and metal oxides that has arisen from non-covalent interactions such as H-bonding or van der Waals interaction.³⁸ The non-covalent functionalization of CoMoO₄ with surfactant made no changes to the chemical structure of the molybdate but provides effective means to tune the electronic properties of the cobalt molybdate.³⁹ For the polymer modified sample, the intensities of the Co (2p) peaks were very low indicating a strong covalent interaction like crosslinking on chitosan matrix and gelation due to acetic (or) citric acid occurs that resulted in a greater cross-linked chain³⁰ while inhibiting the Co species underneath. The degree of functionalization alters the segmental mobility and hence the observed weak intensity of Co (2p) peaks. This is also ascertained from the XPS spectra of C (1s) and O (1s) for the CoMoO₄ samples. Fig. 2b shows the XPS spectra of C (1s) comprising two types of carbon peaks, one at 285 eV assigned to the chemical state (C–C) which are hydrocarbons present in all the samples, and the other at 288.5 eV and 286.3 eV could be assigned to the chemical state of the biopolymer C=O and C–O, respectively⁴⁰ which is seen only for polymer modified CoMoO₄. This is a clear indication that the parent and chemical modified samples don't contain any polymer (surface functional) groups on the surface which is quite reasonable. For the chemical modified CoMoO₄, the presence of cationic surfactant accelerates the carbon deposition on the surface as evidenced from the increment in the intensity for C (1s) peak (Fig. 2b) at 285 eV than the parent sample. However, the extent of

intensity is higher for polymer modified indicating it has more composition of carbon. Likewise, two types of oxygen peaks, one at 530.2 and 531.9 eV corresponding to metal oxides and organic C – O respectively⁴¹ have been seen in (Fig. 2c) the XPS spectra of O (1s). The observed O (1s) spectral characteristics for chemical modified sample is quite distinct having two states of oxygen while only one state of oxygen is observed in Fig. 2c for the as-prepared and polymer modified. This indicates the chemical modified (uncross-linked) CoMoO₄ has metal oxides and carbon composite on the surface layer whereas polymer modified (cross-linked) CoMoO₄ has different surface functionality with organic groups on the near surface regions. This cross-linking provides an effective way to control the interface between CoMoO₄ particles and the adsorption/desorption of ions with which they are designed to interact.⁴² Notably, the differences observed within the polymer modified approach i.e. between acetic and citric acids are quite indistinguishable so it's not been included in the study.

3.2 Morphological studies of CoMoO₄

Microscopic analysis provides vital information on the size and homogeneity of CoMoO₄ modified materials. The Field Emission SEM (FESEM) images of the as-prepared and modified samples are compared in Figs. 3-5.

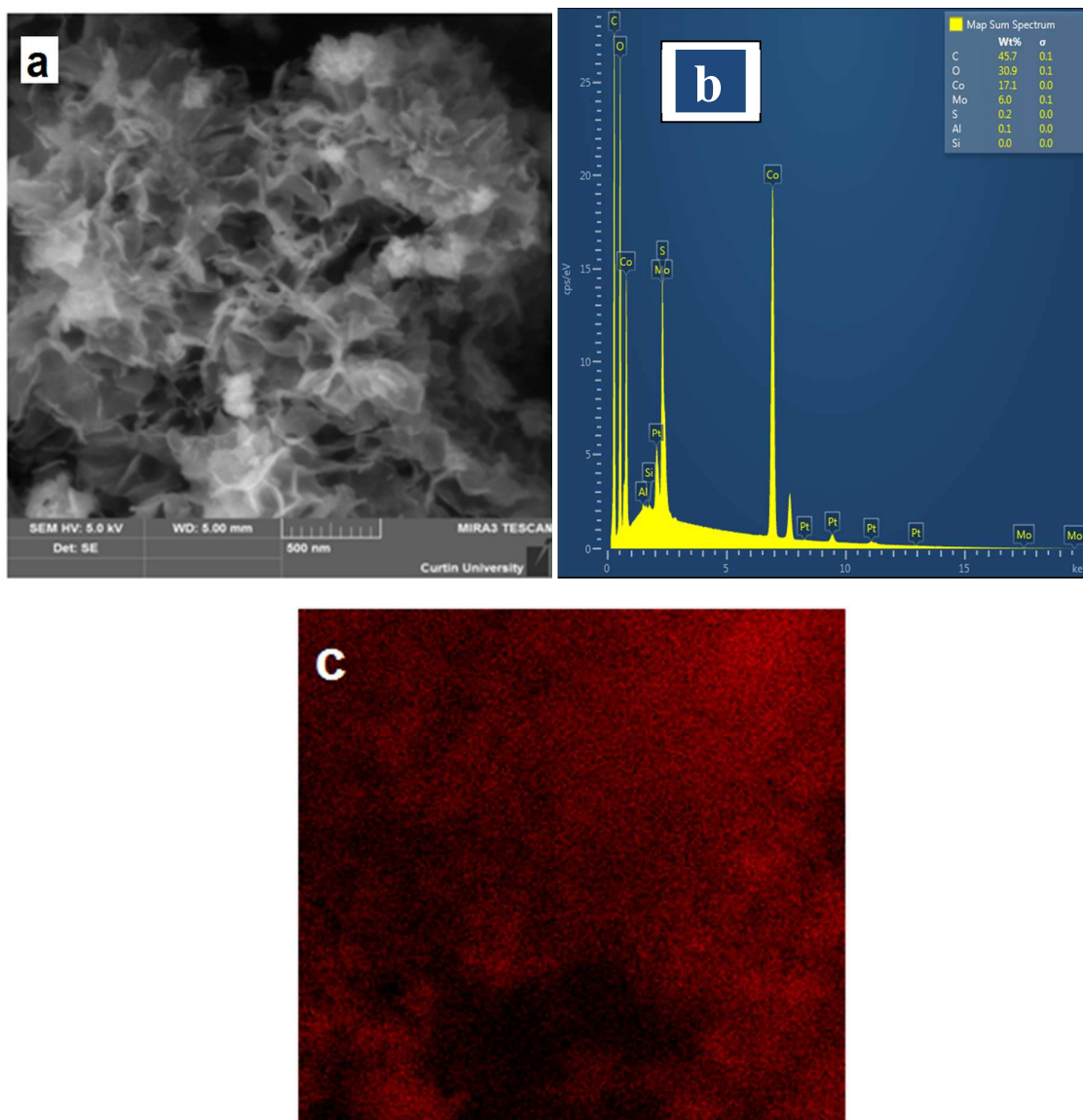


Figure 3 FIB-SEM image of (a) as-prepared CoMoO_4 showing nanosheet like morphology, (b) corresponding elemental dispersive analysis spectra (EDS) and (c) elemental mapping for Carbon.

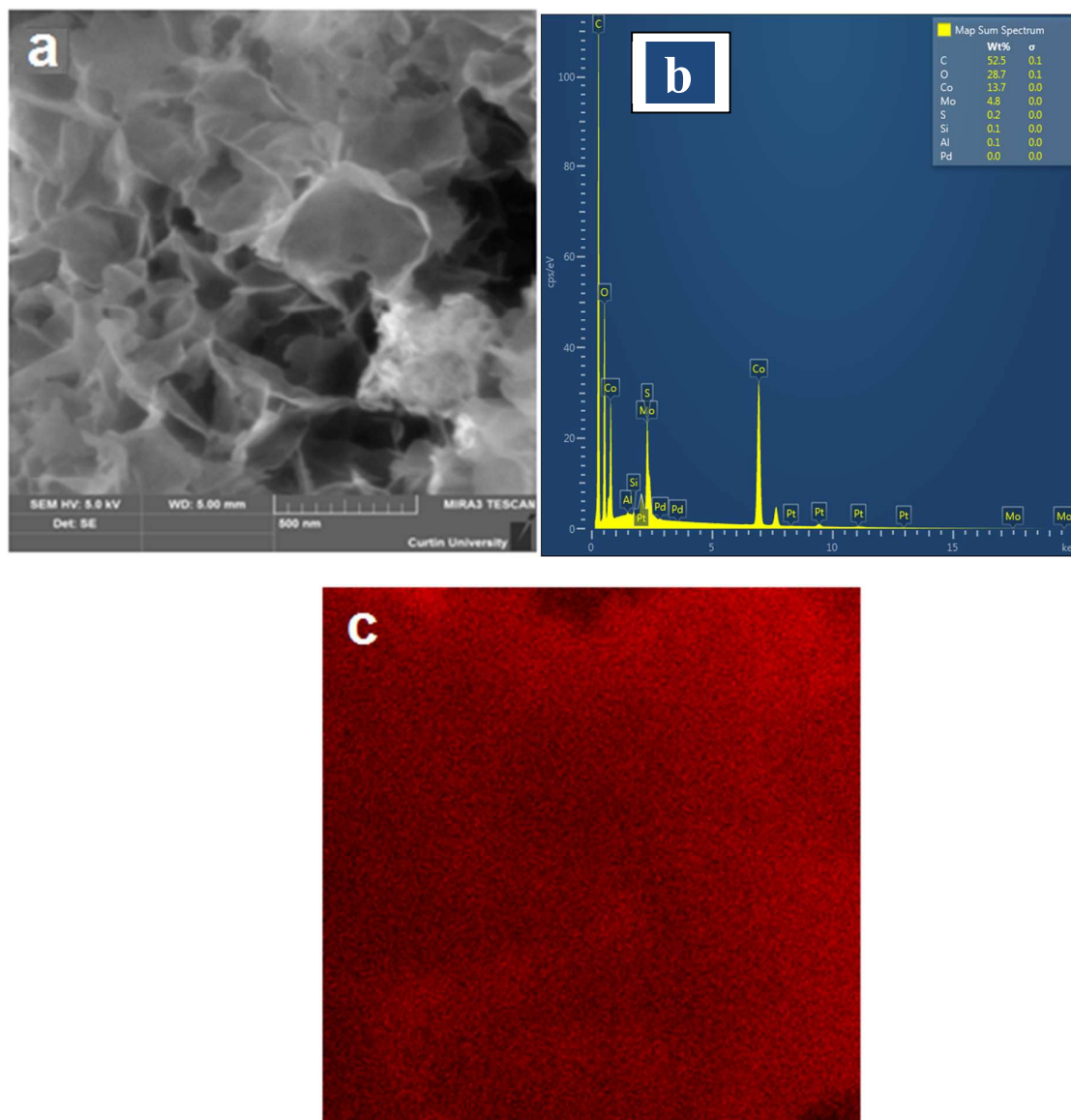


Figure 4 FIB-SEM image of (a) chemical modified CoMoO_4 showing nanoflake like morphology, (b) corresponding elemental dispersive analysis spectra (EDS) and (c) elemental mapping for Carbon.

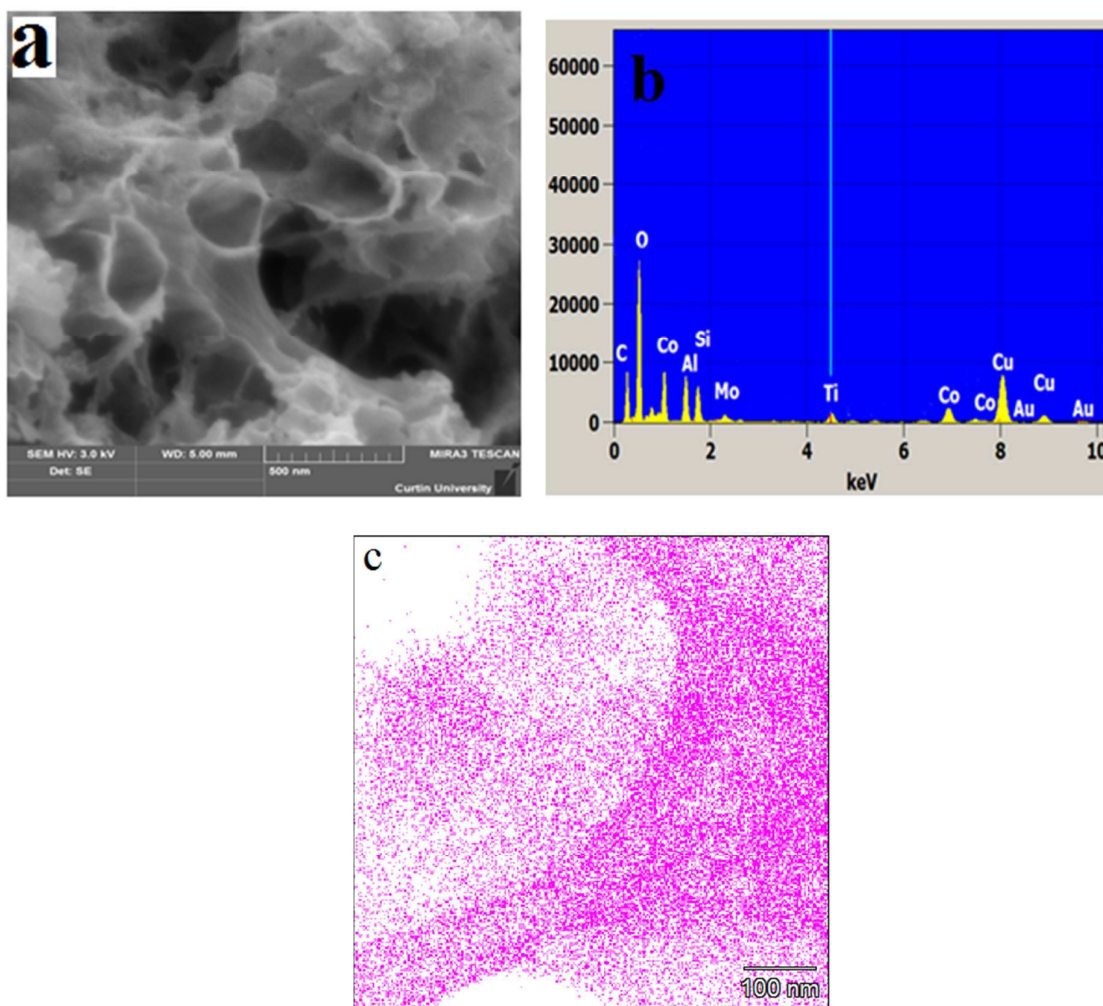


Figure 5 FIB-SEM image of polymer modified CoMoO_4 showing nanowafers like morphology with honey-comb arrangement, (b) corresponding elemental dispersive analysis spectra (EDS) and (c) elemental mapping for Carbon.

The FESEM images show significant morphological variations ranging from nanosheets to nanowafers occurs by the chemical modification method. The as-prepared CoMoO_4 shows (Fig. 3a) nanosheet morphology with mesoporous structure having an edge thickness between 5 and 10 nm while the chemical modified (presence of CTAB) sample shows (Fig. 4a) nanoflake-like structure. CTAB as a cationic surfactant plays a crucial role in controlling the morphology while minimizing the electrostatic repulsive force and leaving carbon composites on the as-prepared material.^{7, 27} This is identified through the SEM images and its

corresponding elemental dispersive spectra (EDS) analysis and carbon elemental mapping. The composition of carbon is found to be more for chemical and polymer modified samples than that of the parent material (compare Figs. 3b-c, 4b-c and 5b-c) illustrating the residual carbon arise from the cationic surfactant and organic citric acid which are supporting the XPS data. The elemental analysis corresponding to CoMoO_4 samples also confirms the presence of mainly Co and Mo. Figure 5 represents the FESEM micrograph of the polymer modified sample showing nanoflake-like particles with honeycomb arrangement having an edge thickness between 2 and 5 nm. The strong interactions between chitosan and citric acid (Chitosan/CA), showed continuous interpenetrating structures, nanoflake like morphology which could provide larger surface area for better adsorption of ions from the aqueous electrolyte.⁴² These observations confirm that grafting citric acid onto biopolymer chitosan gains unique morphology³¹ and particle distribution as well as electrostatic interactions between the couple. It's been reported in the literature⁴³⁻⁴⁶ that stringent synthetic procedure like hydrothermal method need to be used to obtain nanoflakes/wafer like structure but our studies show that conventional one-step solution combustion synthesis would suffice.

The morphological studies are further corroborated with the high resolution TEM analysis associated with selected area diffraction (SADP) technique. The as-prepared CoMoO_4 sample (Fig. 6) has crystalline nature with nanosheet and mesoporous morphology.

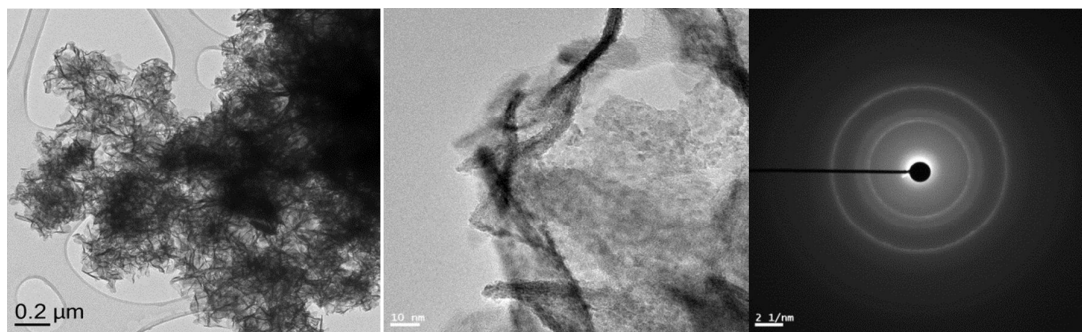


Figure 6 Low magnification bright-field TEM image, high magnification of nanocrystalline region and SADP of as-prepared CoMoO_4 (from left to right).

The high magnification TEM shows a nanocrystalline region in a single grain and the corresponding SADP pattern (in a different area) showed a concentric pattern of rings without significant diffraction spots suggests the formation of fine-grain structures which are not highly crystalline which is supporting the XRD pattern (Fig. 1a) discussed in the earlier section. The combustion method employed in this study assists in the formation of nanocrystalline sizes without any particle agglomeration. The TEM images of the chemical modified CoMoO_4 (Fig. 7) showed fibrous like flaky particles with a reduced particle size and its high magnification image illustrates the regions of nanoparticulates.

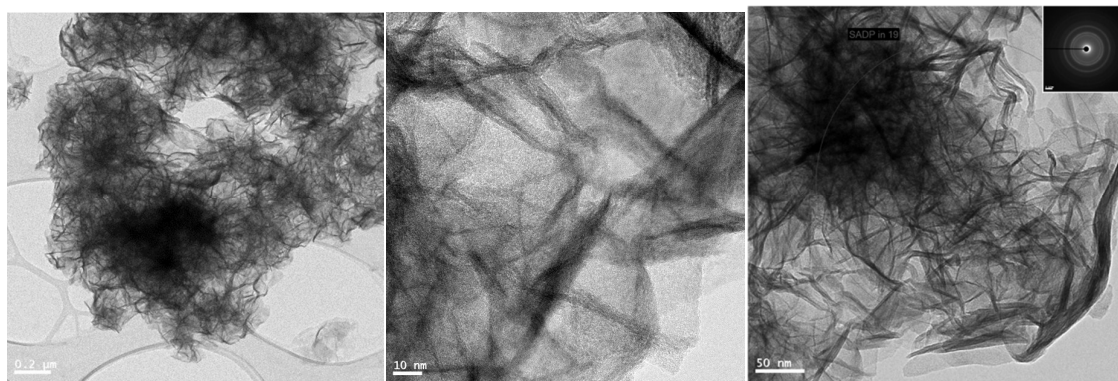


Figure 7 Low magnification bright-field TEM image, high magnification images showing nanocrystalline, nanowafers with SADP for chemical modified CoMoO_4 (from left to right).

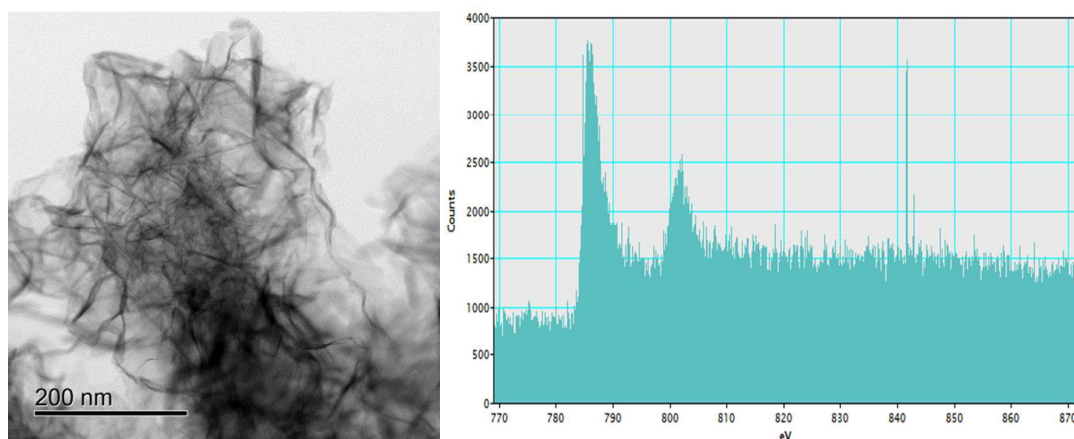


Figure 8 Bright field TEM imaging of chemical modified CoMoO_4 (left) and an EELS spectrum acquired from the corresponding image, Co-L edge fine structure showing the L_3 and L_2 lines.

The bright field image of the chemical modified sample (Fig. 8) shows the region with different contrast. The region having Co^{3+} shows lighter contrast on the edges, and the one with Co^{2+} shows darker contrast implying the distribution of cobalt is having different valence states. Predominantly, the area of the analysis is covered by dark contrast with Co^{2+} state. This is further substantiated by the energy-loss spectroscopy (EELS) spectrum acquired from the area of the bright field image. The Co-L edge of the lines acquired from L_3 and L_2 at 780 and 800 eV regions, based on the lower L_3/L_2 intensity ratio, confirms the presence of cobalt state higher than $2+$ ⁴⁷ asserting the studies of XPS (Fig. 2a) discussed in the earlier section. The TEM images for the polymer modified CoMoO_4 with acetic acid (AA) and citric acid (CA) have been shown in Figs. 9 and 10.

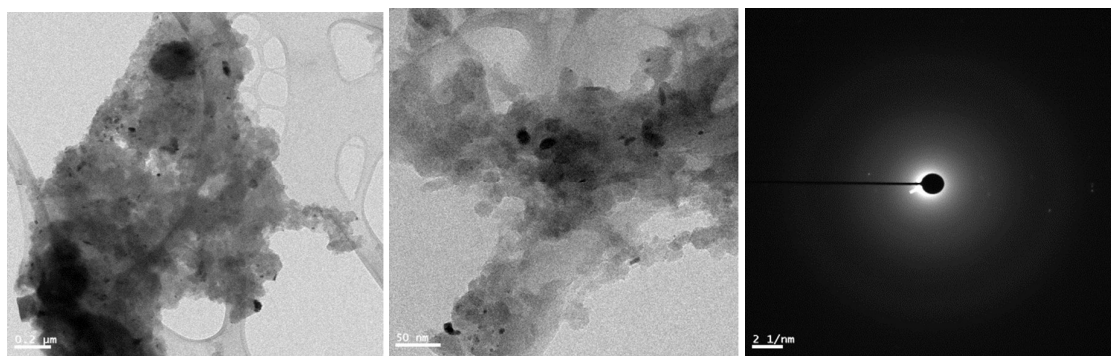


Figure 9 TEM imaging, high magnification of few crystalline region and SADP illustrating diffused rings for polymer modified (AA) CoMoO_4 (from left to right).

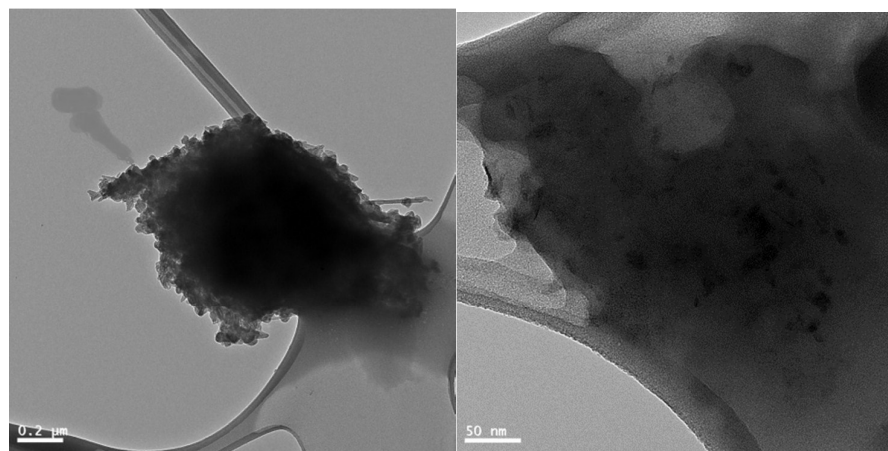


Figure 10 TEM imaging showing nanoparticulate rich region and another region plausibly showing crystalline particles in a gel matrix (Chitosan) for polymer modified (CA) CoMoO_4 (from left to right).

Figure 9 showed very few crystalline regions in an amorphous matrix, SADP pattern of the area illustrating diffused rings indicates grafting didn't occur rather chitosan cross-linked with CoMoO_4 and deteriorated the host structure. Whereas, in the case of citric acid, TEM images in Fig. 10 shows uniform nanocrystalline particulates and the another region showing polymer gel like porous structure with an overall increase in surface area of the matrix. The TEM imaging in Fig. 10 also confirms that CoMoO_4 is well dispersed in the chitosan using citric acid as the medium but this is not the case for weak acetic acid (see Fig. 9). This confirms that chitosan cross-linked with citric acid and grafting occurred while maintaining the CoMoO_4 structural integrity. The proposed conceptual in a schematic view in

Fig. S5 is in accordance with the obtained TEM images on the formation of CoMoO₄/chitosan composite.

All the structural and morphological studies confirm that the chemical and polymer modified CoMoO₄ are quite distinct in terms of surface chemistry. It is expected that the polymer modified material can improve the properties of adsorption/desorption of ions rather the chemical modified that relies on the van der Waals force and other electrostatic interactions which could be less versatile. With this as the background for these materials, an extensive electrochemical investigation has been done to test its suitability for energy storage applications. The role of surfactant and chitosan and its influence in electrochemical property is discussed in the ESI⁸.

3.3. Electrochemical studies of CoMoO₄

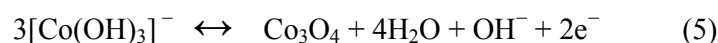
To evaluate the capacitive properties of the as-prepared CoMoO₄ and the modified CoMoO₄, cyclic voltammetry (CV), galvanostatic charge-discharge (CD), and electrochemical impedance spectroscopy (EIS) studies were carried out in 2 M NaOH electrolyte. The two electrode experiment was carried out with activated carbon (*negative electrode*) and CoMoO₄ (*positive electrode*) coated on graphite sheets as a current collector. The cyclic voltametric curves were also run for the blank graphite electrodes, which showed almost negligible current when compared to the active material (CoMoO₄). For the CoMoO₄ vs. AC (cobalt molybdate versus activated carbon) the best electrochemical behaviour was obtained within the applied potential range from 0.2 and 1.5 V. The specific capacitance was calculated from the CV and CD plots by using the following equations:

$$C_s = \frac{1}{vm(V_2 - V_1)} \int_{V_1}^{V_2} i(V)dE \quad (3)$$

$$C = \frac{I \Delta t}{m \Delta V} \quad (4)$$

where V_2-V_1 is the applied potential window, I is the current, m is mass of the active material, and Δt is the discharge time corresponding to the voltage window, ΔV and v the scan rate.

Figs. 11a, 12a, 13a and 14a shows the cyclic voltammetric curves for the as-prepared, chemical modified and polymer modified CoMoO_4 with acetic acid (AA) and citric acid (CA), respectively. The CV plots of as-prepared and polymer modified (AA), Figs. 11a and 13a, show well-resolved peaks comprising one anodic (A_1) but two cathodic peaks (C_1 and C_2) during the positive and negative sweeps. However, a shoulder (A_2) is also seen for as-prepared sample at higher scan rates. In the case of chemical modified and polymer modified (CA), Figs. 12a and 14a, CV plots show only a pair of peaks (A_1 and C_1) during the oxidation and reduction processes. These results suggest that the specific capacitance arising from the as-prepared CoMoO_4 could be dominantly from the redox mechanism involving electron transfer (Faradaic reactions).⁴⁵ The chemical modified CoMoO_4 sample involves both redox (Faradaic reactions) and EDLC mechanism representing quasi-rectangular shapes.¹⁸ The polymer modified one has a different behaviour i.e., the chitosan dissolved in acetic acid in the presence of CoMoO_4 generates a capacitance based on redox reactions but the current is very less in comparison with the CoMoO_4 in citric acid cross-linked chitosan. The Faradaic reactions corresponding to the redox peaks are attributed to the reversible reaction of $\text{Co}^{2+}/\text{Co}^{3+}$. The proposed electrochemical reactions as reported for CoMoO_4 ⁴⁵ are as follows:



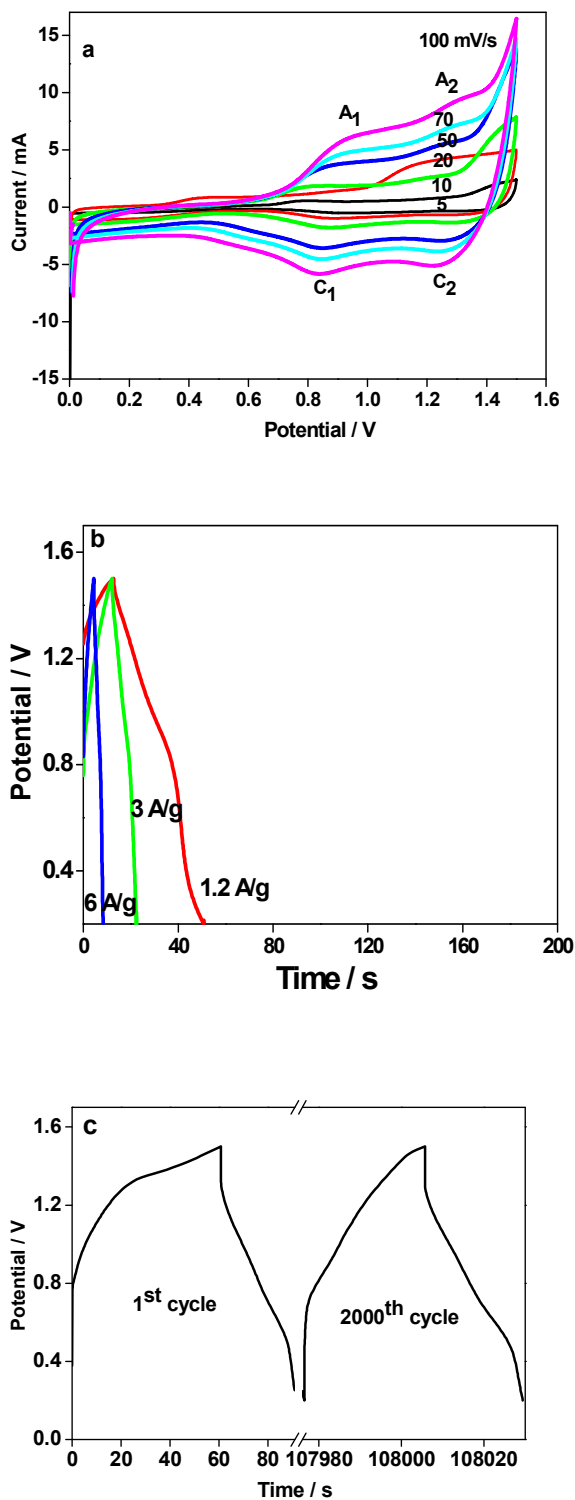


Figure 11 (a) Cyclic voltammetry (CV), (b) Charge – discharge (CD) and (c) long term cycling behaviour of as-prepared CoMoO_4 vs. activated carbon capacitor.

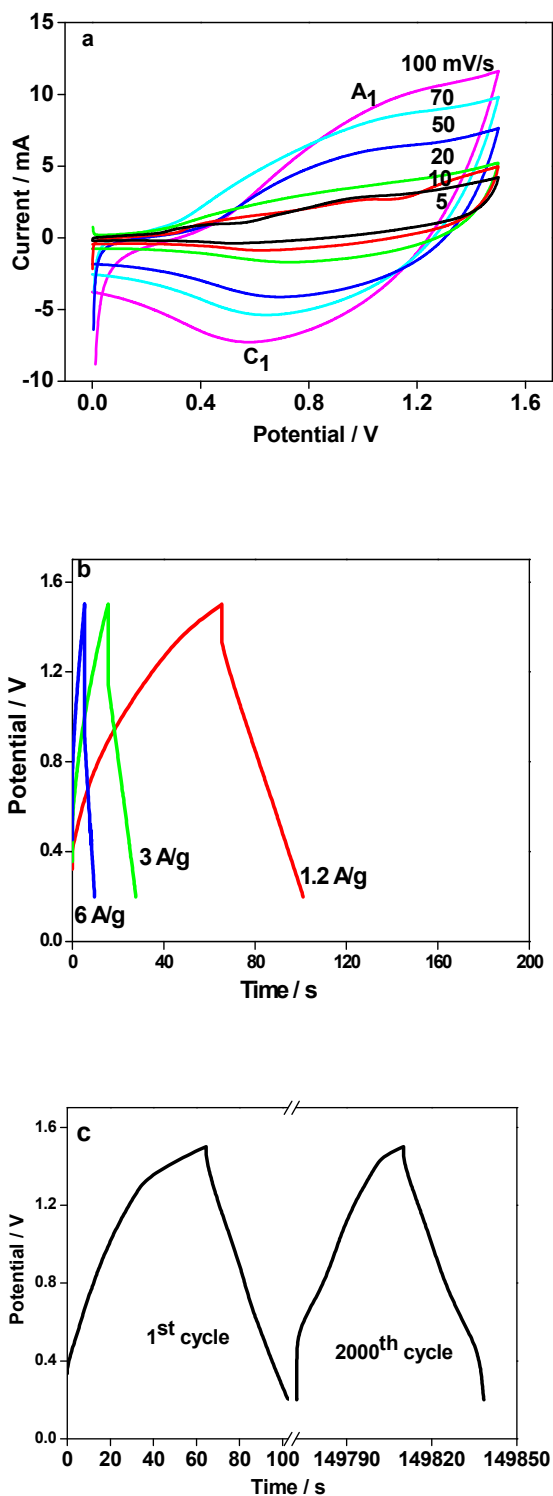


Figure 12 (a) Cyclic voltammetry (CV), (b) Charge – discharge (CD) and (c) long term cycling behaviour of chemical modified CoMoO_4 vs. activated carbon capacitor.

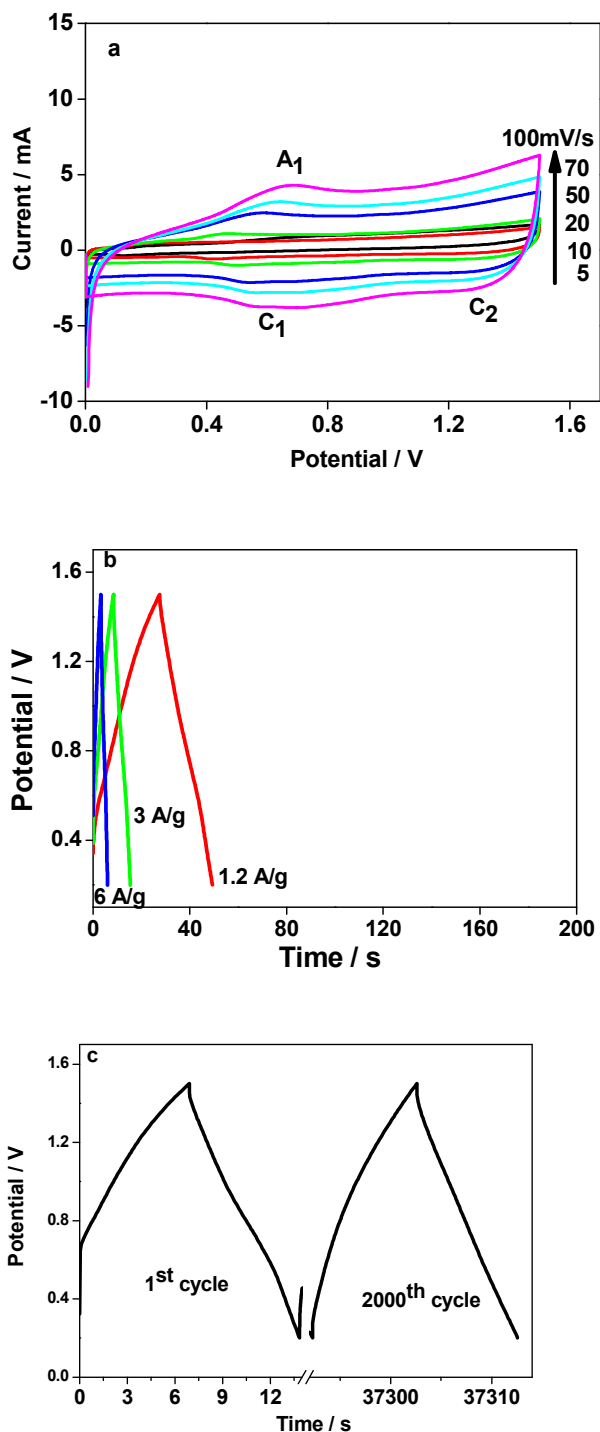


Figure 13 (a) Cyclic voltammetry (CV), (b) Charge – discharge (CD) and (c) long term cycling behaviour of polymer modified (AA) CoMoO₄ vs. activated carbon capacitor.

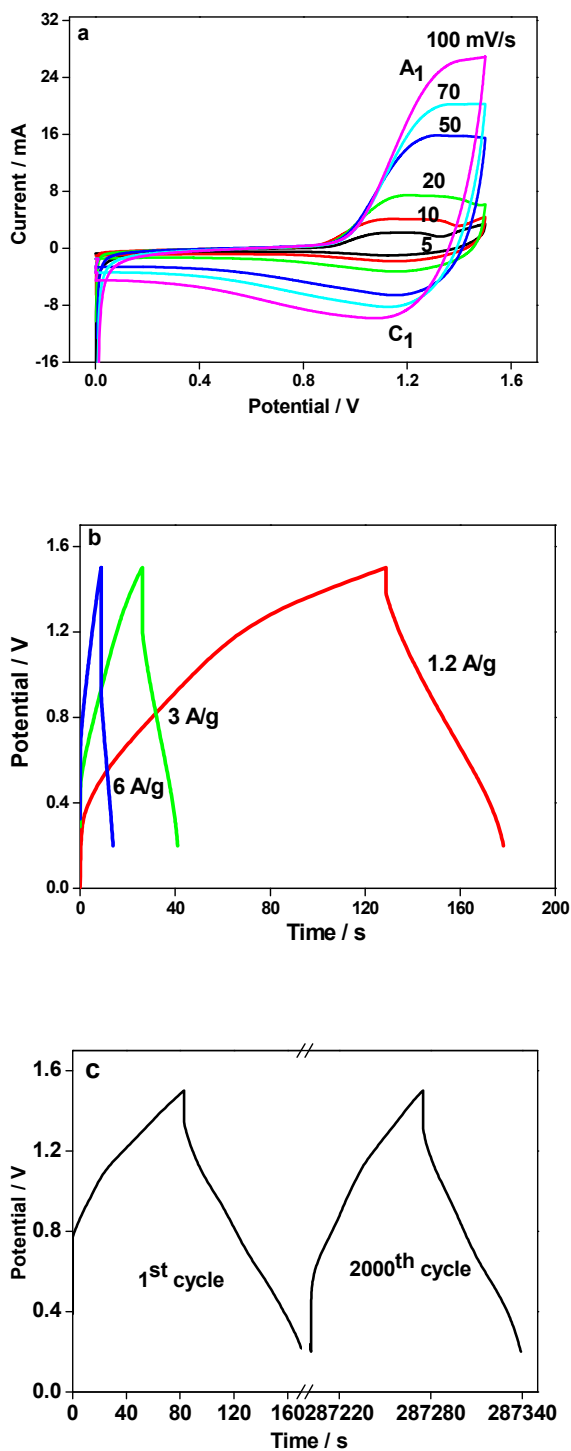


Figure 14 (a) Cyclic voltammetry (CV), (b) Charge – discharge (CD) and (c) long term cycling behaviour of polymer modified (CA) CoMoO₄ vs. activated carbon capacitor.

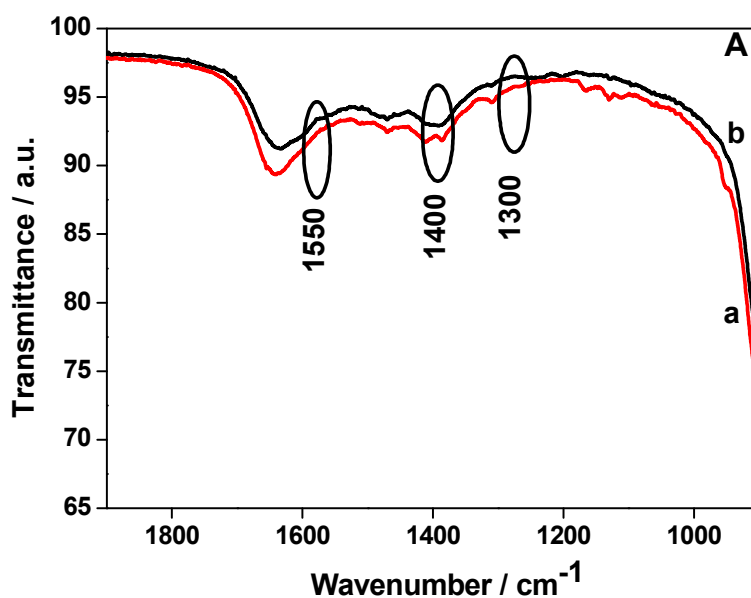
The obtained specific capacitance for the as-prepared and modified CoMoO₄ is tabulated in Table 1. Comparing the CV plots for as-prepared (Fig. 11a) and polymer modified (AA) CoMoO₄ (Fig. 13a), AA showed a poorer capacitance of 39 F/g against 58 F/g at 20 mV/s (see Table 1) with meagre amount of current response (to be noted the scales in the y-axes are different). The grafting didn't occur for Chitosan/AA, but chitosan grafted with the host CoMoO₄, deteriorated the structure, and hence the electrochemical performance has no influence in storage capability resulting in poor specific capacitance. At higher scan rates the available capacitance for AA is even lower (27 F g⁻¹ at 100 mV s⁻¹) than the as-prepared material (see Table 1).

Table 1 Specific capacitance of CoMoO₄ materials obtained through potentiodynamic (CV) method at different sweep rates

Scan rate (mV/s)	as-prepared (F/g)	chemical modified (CTAB) (F/g)	polymer modified (AA) (F/g)	polymer modified (CA) (F/g)
5	56	148	73	177
10	54	93	47	105
20	58	76	39	92
50	42	53	33	71
70	36	51	29	60
100	32	39	27	50

The current response and the obtained capacitance for the polymer modified CA sample (Fig. 14a) are higher than the chemical counterpart (Fig. 12a) exhibiting 92 F/g against 76 F/g at 20 mV/s. The increase in current at higher scan rates (Fig. 14a) is found to be more linear for the polymer modified (CA), indicating the ease of Faradaic mechanism at

the interface between the electrode and electrolyte.⁴⁸ The current increased in a linear fashion with square root of scan rate for both chemical and polymer modified CoMoO₄ samples (Figs. 12a and 14a) indicating diffusion controlled reaction. The obtained capacitance is directly proportional to the applied current at various scan rates and a maximum value is achieved (177 F/g at 5 mV/s) for the polymer modified (CA) in Fig. 14a, confirming the reversible kinetics of the electron and ionic transfer.⁴⁸ The enhanced electrochemical performance is supported by the surface chemistry of the CoMoO₄ analysed by the FTIR spectra shown in Fig. 15. The citric acid (CA) has three COOH groups in comparison with acetic acid (AA), which has only one carboxylic acid moiety.³¹ Those COOH band variations between 1300 and 1550 cm⁻¹ between AA and CA have been shown in the mid infrared region shown in Fig. 15B. A similar kind of COOH bands are not viewed in the respective locations for as-prepared and chemically modified CoMoO₄ (Fig. 15A) which is quite reasonable as there is no cross-linker present in those samples.



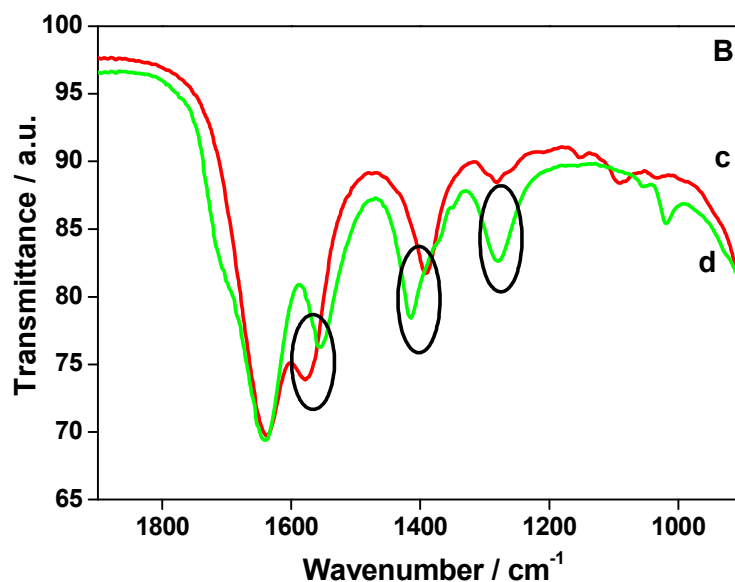


Figure 15 Infrared spectra of CoMoO₄. (A) as-prepared (a) and chemical modified (b) CoMoO₄ samples. (B) Polymer modified CoMoO₄; chitosan dissolved in (c) acetic acid and (d) citric acid.

The presence of more COOH ensures that the Chitosan/CA can be cross-linked without the aid of any external cross-linking agent like glutaraldehyde.³⁰ Moreover, as verified by XPS and TEM analyses, the surface chemistry of CoMoO₄ was enhanced by the transfer of charges generated by the surface functionality and the molybdate moieties on the surface.⁴⁹ The charge storage of chemical (CTAB) and polymer (Chitosan/CA) modified samples are dominated by surface-confined capacitance rather than by Na⁺ ion or H⁺ insertion. This conceptual is well supported by the observed electrochemical behaviour in Figs. 12a and 14a based on the small peak separation (0.5V for chemical 0.25V for polymer CA), marginal changes in the cathodic peak shift (~ 0.2 V) and proportional current response at higher scan rates. The observed higher current response in turn securing maximum specific capacitance of 177 F/g at 5 mV/s for polymer modified electrodes is due to the unique nanowafers like

morphology that reduces the diffusion lengths for the electrolyte ions and improves the reversibility.^{18,22} Although nanosheets are attractive candidates for capacitive properties but nanowafers form a loose honey-comb like arrangement that gains penetration of ions on both sides of surface and hence effectively enhancing the specific capacitance.

To further understand the capacitive behaviour of CoMoO₄ and to examine the suitability for energy storage device, we investigated the galvanostatic charge/discharge analyses. The charge/discharge behaviour for the as-prepared, chemical and polymer modified CoMoO₄ is carried out at three different current densities, i.e., 2, 5 and 10 mA cm⁻² within the safe voltage window between 0.2 and 1.5 V and their results are displayed in Figs. 11b, 12b, 13b, and 14b and Table 2.

Table 2 Specific capacitance of CoMoO₄ materials obtained through galvanostatic charge-discharge studies at different current densities

Current Density (mA/cm²)	as-prepared (F/g)	chemical modified (CTAB) (F/g)	polymer modified (AA) (F/g)	polymer modified (CA) (F/g)
1	39	47	28	75
2	24	39	23	71
5	22	33	18	52
10	20	23	14	42

The as-prepared compound exhibited asymmetric behaviour, which is in accordance to the behaviour seen in CV plots (compare Fig. 11a and Fig. 11b) implying pseudocapacitive feature (plateau like curve) at 0.5 V region. This illustrates an electron transfer occurs in the bulk CoMoO₄ material. The calculated specific capacitance for this material is 22 F/g at a current density 5 mA cm⁻². This is reasonably comparable to the reported values for the

asymmetric capacitor devices based on CoMoO₄ vs. activated carbon.^{23,50} The charge/discharge curves obtained for chemical and polymer modified electrodes including AA and CA (Figs, 12b, 13b and 14b) all appear to be symmetrical, however, polymer modified samples (Figs. 13b and 14b) shows triangular in shape without much ohmic drop indicating improved charge transport. A triangular shape implies a capacitive behaviour and those charge and discharge curves are characterised by single stage, gradual upward potential during charge and slow potential decay during discharge without any visible plateau like region. The calculated specific capacitances for chemical, polymer modified AA and CA are 33, 18 and 52 F g⁻¹ at 5 mA cm⁻² respectively. The specific capacitance calculated for the Chitosan/CA at different current densities 2, 5 and 10 mA cm⁻² is 71, 52 and 42 F g⁻¹. The decrease in specific capacitance at higher current density appears to be quite less (see Table 2) to that of other CoMoO₄ electrodes. The presence of the chitosan moiety does not affect the host CoMoO₄ compound rather Chitosan/CA acts a buffer that greatly improved the reversibility of redox ions. This is due to strong covalent interactions which were created on the molybdate surface because of the grafting of Chitosan/CA.³⁰⁻³¹ The long term charge-discharge performance has been carried out on all the CoMoO₄ samples (as-prepared, chemical and polymer modified) and their results are compared for the first and 2000th cycles in Figs. 11c, 12c, 13c and 14c, respectively. Even after 2000 cycles, nearly symmetrical behaviour confirms the excellent capacitive behaviour of the device and hence form a suitable candidate for renewable energy storage applications. Among the electrodes studied, Chitosan/CA showed the superior performance with excellent cycling stability having capacity retention of 81%. To the best of our knowledge, the specific capacitance of 71 F g⁻¹ at 2 mA cm⁻² (1.2 A/g) has not been reported for CoMoO₄, however, similar values are reported for asymmetric capacitor device but based on NiO vs. activated carbon with an alkaline polymer electrolyte (73.4 F g⁻¹).⁵¹

Only quite few studies have been dealt with the capacitive properties of CoMoO_4 vs. activated carbon in terms of charge-discharge behaviour and long term cycling stability.⁵⁰ Those studies have reported rather low capacitance around 25 F g^{-1} , far from the reported value of our current work. This is likely due to the unique biopolymer approach done by the grafting of chitosan in the presence of citric acid as a crosslinking agent. To evaluate the long term performance of the asymmetric device, the electrodes were employed for multiple cycling at 2 mA cm^{-2} up to 2000 cycles. Fig.16c shows the capacity retention over 2000 cycles. It is clearly seen that, polymer modified (CA) exhibits the highest specific capacitance with an excellent retention 81% of the initial capacitance. In the case of as-prepared and chemical modified samples, (figs. 16 a –b), the retention was 58% and 62% respectively. The

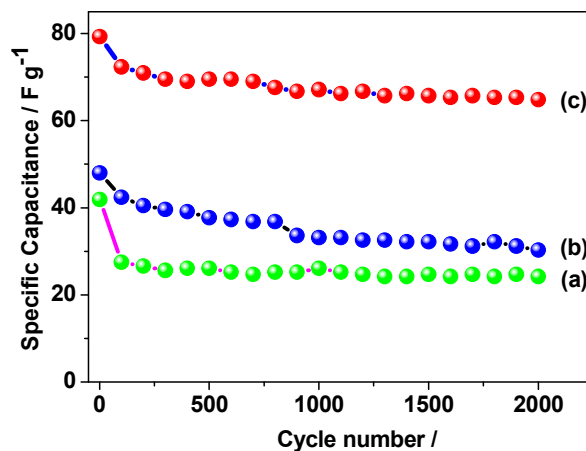


Figure 16 Variation of the specific capacitance vs. the cycle number at a rate of 1.2 A/g for the (a) as-prepared, (b) chemical and (c) polymer modified CoMoO_4 .

higher capacitance retention implies the effective cross-linking strategy occurred in the presence of citric acid as a cross-linker without any aid of conventional glutaraldehyde.²⁴ The high current response of the polymer modified CoMoO_4 was also exhibiting excellent high energy density of 18 Wh kg^{-1} . Figure 17 show the energy density plot for CoMoO_4

electrodes and the obtained energy density was higher for Chitosan/CA with a maximum energy density value of 18 Wh kg^{-1} .

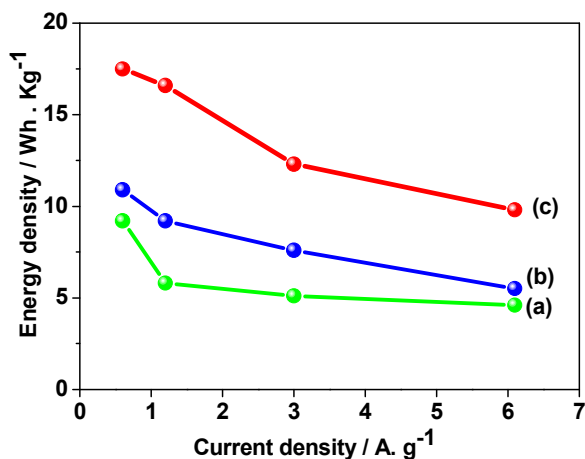


Figure 17 Plot of energy density vs. current density for the (a) as-prepared, (b) chemical and (c) polymer modified CoMoO_4 electrodes.

Electrochemical impedance spectroscopy (EIS) was carried out in order to further ascertain the capacitive behaviour of the as-prepared, chemical and polymer modified CoMoO_4 electrodes. The impedance measurements were performed from 0.01 to 200 kHz at an open circuit potential with amplitude of 10 mV. The Nyquist plots for CoMoO_4 electrodes are shown in Figure 18.

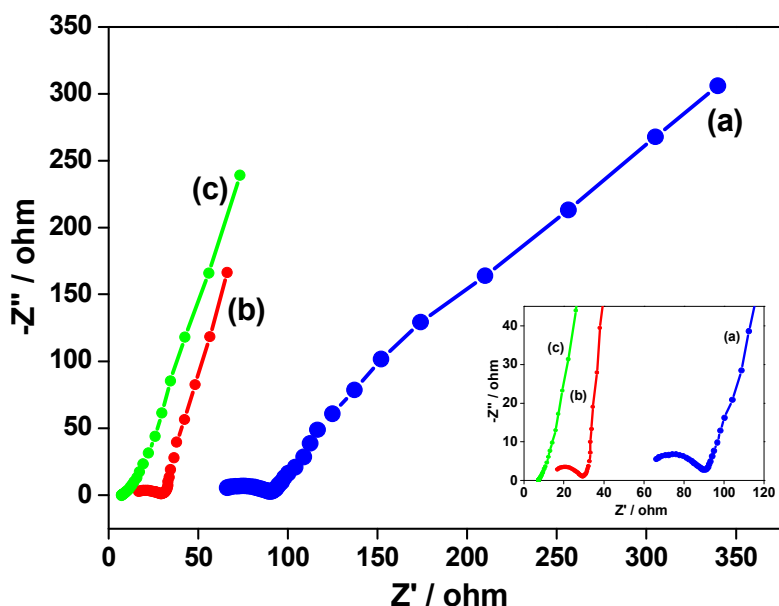


Figure 18 Nyquist plots for the (a) as-prepared, (b) chemical and (c) polymer modified CoMoO_4 electrodes.

The Nyquist plot represents the way of showing frequency responses of the electrode/electrolyte interface while examining the imaginary component ($-Z''$) of the impedance compared to the real component (Z').⁵² The typical plots for the CoMoO_4 electrodes are shown in Fig. 18, showing a tiny semicircle region at the high-frequency and a linear section at the low-frequency which is quite similar in behaviour to that reported in the literature.⁵³ The diameter of the semicircle in the plot indicates the charge transfer resistance (R_{ct}) for the as-prepared, chemical and polymer modified electrodes (Fig. 18 a-c) and the obtained values were 32, 16 and 2 Ω respectively. The polymer CoMoO_4 exhibits no semicircle in the high frequency region as opposed to the behaviour shown by chemical and as-prepared materials indicating higher faradaic resistance. The as-prepared CoMoO_4 has a semicircle at high frequency region with high solution resistance indicates high resistance with a low conductivity than the chemical and polymer modified sample. A low frequency

spiked line, referred to as the Warburg resistance (Z_w) used to mimic the behavior of diffusion of OH^- ions. The low frequency inclined line shows the as-prepared sample (Fig. 18a) may have difficulty for OH^- ions diffusion from the electrode/electrolyte interface to the bulk CoMoO_4 . The more linear the straight line illustrates the higher the capacitive nature of the material indicating adsorption/desorption mechanism is favoured for the chemical and polymer modified samples (Fig. 18b-c) through the electrode/electrolyte interface. The lower solution resistance and lower slope of polymer modified sample indicates the faster OH^- ion diffusion of electrolyte than the as-prepared and chemical modified electrodes. Here the typical equivalent circuit consists of a solution resistance (R_s), charge transfer resistance (R_{ct}), Warburg resistance (Z_w) and a constant phase element (CPE) which can model the behaviour of the asymmetric capacitor. The obtained impedance values are in good agreement with the other electrochemical measurements discussed earlier.

3.4. Electrochemical studies of CoMoO_4 in solid state polymer electrolyte

A solid state asymmetric capacitor based on Chitosan/CA conducting polymer gel electrolyte while replacing the conventional 2M NaOH “liquid” electrolyte is fabricated. The solid state asymmetric device is based on CoMoO_4 | Chitosan/CA | AC and its preliminary electrochemical results are reported in Fig. 19.

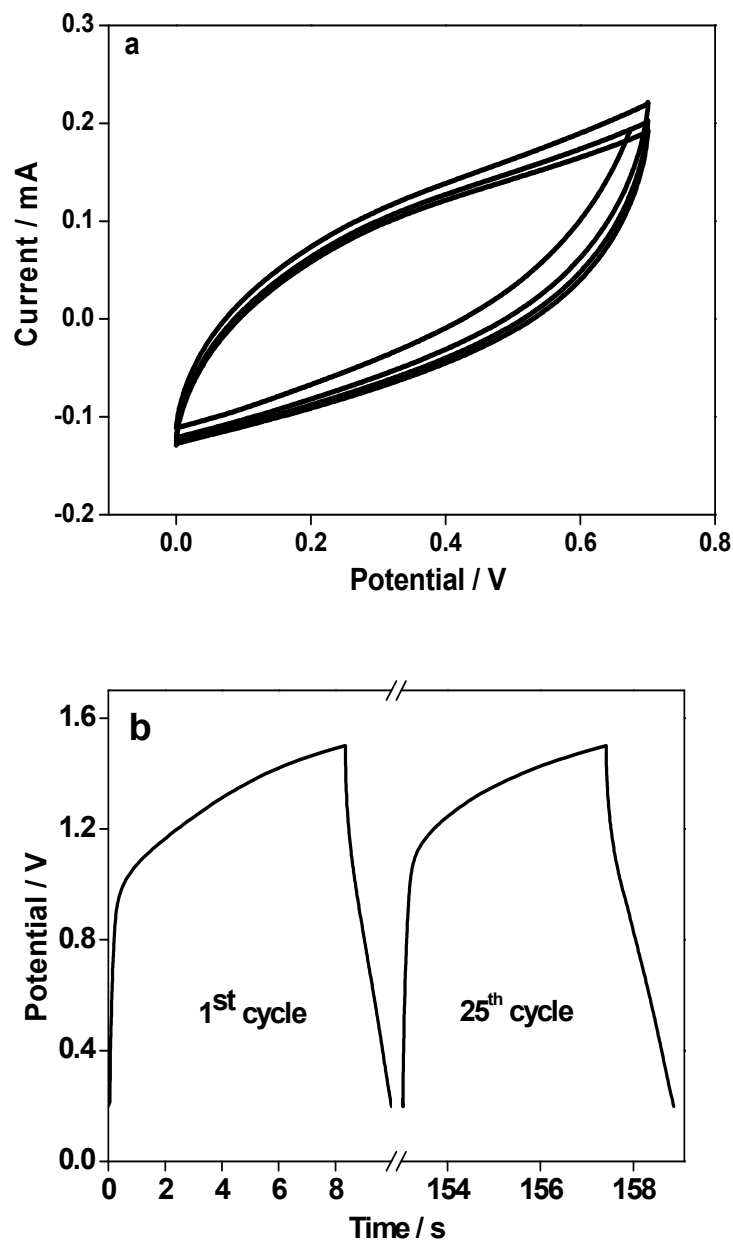


Figure 19 Cyclic voltammetry (a) and charge-discharge (b) plots of the solid state capacitor type CoMoO_4 | Chitosan/CA | AC, at a current of 6 A/g.

The typical CV plot in Fig. 19 represents an ideal capacitive behaviour without any defined redox peaks.¹⁸ A capacitor based on biopolymer gel electrolyte closely mimics an EDLC mechanism, representing a non-faradaic reaction occurred during the electrochemical

processes. Due to the poor electrode-electrolyte contact, the charge – discharge behaviour of the device gave us a significantly low specific capacitance of just 10 F g^{-1} . The use of solid state (gel) electrolyte may have some advantages but our biopolymer approach using liquid electrolyte performed in an excellent manner so using Chitosan/CA as a gel electrolyte wouldn't be a feasible approach. Nevertheless, the obtained low capacitance for solid state device is expected and similar values are well reported in the literature.⁵⁴⁻⁵⁵ For our future studies, efforts will be taken to test these materials in a Swagelok type cell configuration where the electrode-electrolyte contacts can be improved through external pressure applied over the cell.

4. Performance overview of the CoMoO_4 vs. AC capacitor

To summarise, comparison of the cyclic voltammetric curves for the as-prepared, chemical and polymer modified CoMoO_4 samples are displayed in figure 20.

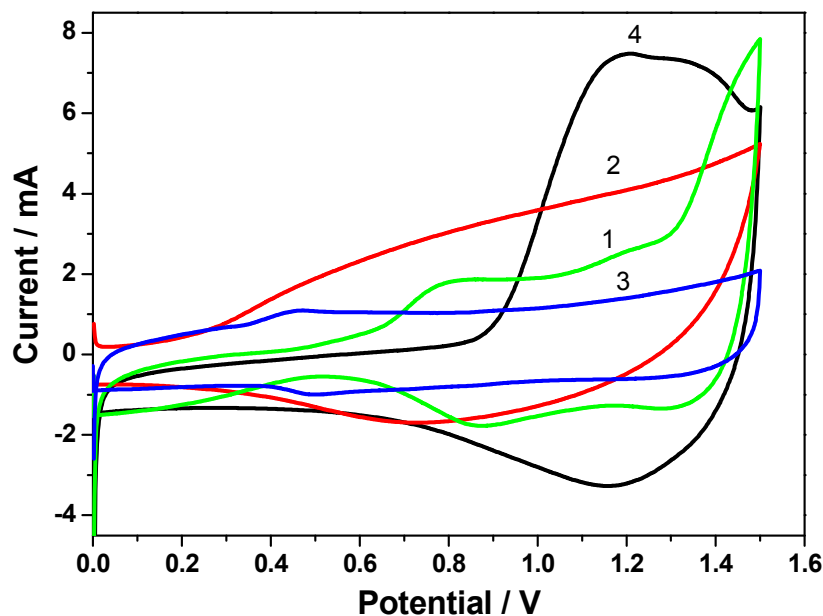


Figure 20 Cyclic voltammetric curves of (1) as-prepared, (2) chemical modified, (3) polymer modified AA and (4) polymer modified CA CoMoO_4 samples scanned at 10 mV s^{-1} .

All the samples exhibit reversible behaviour. The as-prepared CoMoO_4 showed redox peaks at 0.7 and 0.8 V, arising from the oxidation and reduction of $\text{Co}^{2+}/\text{Co}^{3+}$ species on the electrode. This redox (faradaic reactions) behaviour is less clear for the chemical modified CoMoO_4 while it shows an EDLC behaviour (non-faradaic reactions) arising due to the presence of carbon species from the surfactant CTAB moiety. In the case of polymer modified, Chitosan/AA modified CoMoO_4 , set of redox peaks due to the $\text{Co}^{2+}/\text{Co}^{3+}$ is observed but at less positive potentials (0.4 V region) than that of the as-prepared compound. This is an indication illustrating the fact that chitosan/AA interfered with CoMoO_4 and disintegrated the host. Whereas, in the case of chitosan/CA modified CoMoO_4 exhibits redox behaviour with the peaks shifted to more positive potentials at 1.0 V region. This confirms the cross-linking of the polymer occurred in CoMoO_4 and the CA acted as suitable crosslinking agent in solubilizing chitosan with an improved electrochemical behaviour (area under the curve for this sample in Fig. 20 shows a well-defined redox peaks having high current).

Most of the studies reported in the literature are dealt with three electrode system and only few studies have been reported in two electrodes i.e. CoMoO_4 vs. activated carbon.^{23, 26,50} To the best of our knowledge, chemical and polymer modified CoMoO_4 extended to solid state electrolyte has not been reported yet. Few examples of molybdate, oxide and phosphate based electrode materials and their electrochemical performances in aqueous electrolytes are compared with our obtained results in Table 3.

Table 3 Various molybdates and oxides employed in supercapacitor device in a range of aqueous electrolytes and their energy storage performances. The reported specific capacitance is primarily obtained at a galvanostatic (charge-discharge) method at a current density of 2 mA cm^{-2}

Electrodes used in a capacitor device	Specific capacitance (F g^{-1})	Energy density (Wh kg^{-1})	Reference
Activated Carbon 2M KOH Activated carbon	20	5	[26]
$\text{CoMoO}_4\text{-NiMoO}_4 \cdot x\text{H}_2\text{O}$ 2M KOH Activated carbon	80	17	[26]
CoMoO_4 1M NaOH Reduced Graphene Oxide	26	8	[50]
CoMoO_4 2M KOH 3D Graphene	N/A	14.5	[56]
$\alpha\text{-CoMoO}_4$ 2M LiOH Activated carbon	55	14.5	[23]
MnO_2 Polymer electrolyte Activated carbon	48	N/A	[57]
NaMPO_4 2M NaOH Activated carbon	45	15	[58]
$\text{Co}_3\text{O}_4@ \text{CoMoO}_4$ 2M KOH Activated carbon	74	19	[59]
CoMoO_4 - Chitosan 2M NaOH Activated carbon	71	18	This work

It is quite clear from the table 3 that symmetric capacitors (Ac vs Ac) exhibited a low capacitance of 20 F g^{-1} and low energy density of 5 Wh kg^{-1} delivered from EDLC mechanism. However, the asymmetric hybrid devices showed an improved capacitance and energy density resulted from redox mechanism. Apart from the hydrated $\text{CoMoO}_4\text{-NiMoO}_4$ composites²⁶ listed in table 3, our currently reported work is comparable and exhibited a superior electrochemical performance to the remaining work listed thereon.^{23, 26, 50, 56-59} This could be mainly attributed to the synergistic contribution of both nanowafer like morphology with increased ion diffusion and fast electron transport.

5. Conclusions

We have synthesized cobalt molybdate (CoMoO_4) nanosheets via one-step method using solution combustion technique. Two different approaches (chemical and polymer) have been made on CoMoO_4 with the aid of cationic surfactant CTAB and biopolymer chitosan. Nanoflake like morphologies have been prepared using chemical and polymer modified CoMoO_4 materials. CTAB helps in controlling the aggregation and leaving a carbon residual which eventually increased the specific capacitance from 22 F g^{-1} to 33 F g^{-1} at 3 A g^{-1} . The polymer modified CoMoO_4 with Chitosan/CA exhibited a maximum specific capacitance of 71 F g^{-1} at 2 A g^{-1} . Molybdate moiety has been proven to be a potential host for accommodating the chitosan molecule, which strongly adheres to the molybdate. The uncrosslinked sample (Chitosan/AA) showed inferior capacitive properties, substantiating the effective cross-linking strategy for grafting of Chitosan/CA which suits long term cyclability and high adsorption/desorption of ions from the electrolyte. The role of surfactant and chitosan with different crosslinking agents (AA/CA) onto CoMoO_4 were discussed. The grafting effect was confirmed by the structural and morphological (XRD, XPS, SEM and TEM) studies. A biopolymer gel decorated cobalt molybdate nanowafer as an electrode for energy storage device is a novel approach with a specific capacitance of 71 F g^{-1} having energy storage of 18 Wh kg^{-1} .

Acknowledgements

This research was supported under ARC's Discovery Projects funding scheme (DP1092543) and AINSE Research Award ALNGRA15051. The views expressed herein are those of the authors and are not necessarily those of the Australian Research Council. This research used equipment funded by the Australian Research Council (ARC) – Linkage, Infrastructure, Equipment and Facilities (LIEF) grant LE120100104 located at the UOW Electron

Microscopy Centre. Authors greatly acknowledge Dr David Mitchell from UoW for TEM analysis.

References

1. Y. Y. Liang, Y.G. Li, H.L. Wang and H. J. Dai, *J. Am. Chem. Soc.*, 2013, **135**, 2013 – 2036.
2. S. Park, Y. Y. Shao, J. Liu and Y. Wang, *Energy Environ. Sci.*, 2012, **5**, 9331 – 9344.
3. Z. L. Wang, D. Xu. J. J. Xu and X. B. Zhang, *Chem. Soc. Rev.*, 2014, **43**, 7746 – 7786.
4. A. G. Pandolfo and A. F. Hollenkamp, *J. Power Sources*, 2006, **157**, 11 – 27.
5. B. E. Conway, *Electrochemical Supercapacitors – Scientific Fundamentals and Technological Applications*, Kluwer, New York, 1999.
6. N. L. Wu, S. L. Kuo and M. H. Lee, *J. Power Sources*, 2003, **104**, 62 – 65.
7. D. Ghosh, S. Giri and C. K. Das, *ACS Sustainable Chem. Engg.*, 2013, **1**, 1135 – 1142.
8. K. W. Nam, K. H. Kim, E. S. Lee, W. S. Yoon, X. Q. Yang, K. B. Kim, *J. Power Sources*, 2008, **182**, 642 – 652.
9. Q. Abbas, P. Ratajczak and F. Beguin, *Faraday Discuss.*, 2014, **172**, 199 – 214.
10. L. Q. Mai, F. Yang, Y. L. Zhao, X. Xu, L. Xu and Y.Z. Luo, *Nature Commun.*, 2011, **2**, Article 381/1 – 381/5.
11. C. Masquelier and L. Croguennec, *Chem. Soc. Rev.*, 2013, **113**, 6652 – 6591.
12. M. Minakshi, S. Duraisamy, P. R. Tirupathi, S. Kandhasamy, and N. Munichandraiah, *Int. J. Electrochem. Sci.*, 2014, **9**, 5974 – 5992.
13. L. Z. Fan and J. Maier, *Electrochem. Commun.*, 2006, **8**, 937 – 940.
14. K. Naoi, S. Suematsu and A. Manago, *J. Electrochem. Soc.*, 2000, **147**, 420 – 426.

15. Y. R. Ahn, M. Y. Song, S. M. Jo, C. R. Park and D. Y. Kim, *Nanotechnology*, 2006, **17**, 2865 – 2869.
16. J. Jiang and A. Kucernak, *Electrochim. Acta*, 2002, **47**, 2381 – 2386.
17. P. A. Nelson and J. R. Owen, *J. Electrochem. Soc.*, 2003, **150**, A1313 – A1317.
18. G. Wang, L. Zhang and J. Zhang, *Chem. Soc. Rev.*, 2012, **41**, 797 – 828.
19. G. Han, Y. Liu, L. Zhang, E. Kan, S. Zhang, J. Tang and W. Tang, *Sci. Reports*, 2014, **4**, Article 4824/1 – 4824/7.
20. M. Sathish, S. Mitani, T. Tomai and I. Honma, *J. Mater. Chem. A*, 2011, **21**, 16216 – 16222.
21. L. L. Yu, J. J. Zhu and J. T. Zhao, *J. Mater. Chem. A*, 2014, **2**, 9353 – 9360.
22. G. K. Veerasubramani, K. Krishnamoorthy, S. Radhakrishnan, N. J. Kim and S. J. Kim, *Int. J. Hydrogen Energy*, 2014, **39**, 5186 – 5193.
23. S. Baskar, D. Meyrick, K. Ramakrishnan and M. Minakshi, *Chem. Engg. J.*, 2014, **253**, 502 – 507.
24. R. Ramkumar and M. Minakshi, *Dalton Trans.*, 2015, **44**, 6158 – 6168.
25. K. S. Park, S. D. Seo, H. W. Shim, and D. W. Kim, *Nanoscale Res Lett.*, 2012, **7**, 35 – 41.
26. M. C. Liu, L. B. Kong, C. Lu, X. J. Ma, X. M. Li, Y. C. Luo and L. Kang, *J. Mater. Chem. A*, 2013, **1**, 1380 – 1387.
27. B. Tah, P. Pal, M. Mahato and G. B. Talapatra, *J. Phys. Chem. B*, 2011, **115**, 8493 – 8499.
28. L. Bekale, A. Agudelo, H. A. Tajmir – Riahi, *Colloids and Surfaces B: Bio interfaces*, 2015, **125**, 309 – 317.
29. G. Romanazzi, F. M. Gabler, D. Margosan, B. E. Mackey and J. L. Smilanick *Phytopathology*, 2009, **99**, 1028 – 1036.

30. S. M. Gawish, S. M. Abo El-Ola, A. M. Ramadan and A. A. Abou El-Khier, *J. Appl. Polymer Sci.*, 2012, **123**, 3345 – 3353.
31. I. Yamaguchi, S. Iizuka, A. Osaka, H. Monma and J. Tanaka, *Colloids and Surfaces A: Physicochem. Eng. Aspects*, 2003, **214**, 111 – 118.
32. J. Shi, H. Hu, Y. Xia, Y. Liu and Z. Liu, *J. Mater. Chem. A*, 2014, **2**, 9134 – 9141.
33. N. A. Choudhury, P. W. C. Northrop, A. C. Crothers, S. Jain and V. R. Subramanian, *J. Appl. Electrochem.*, 2012, **42**, 935 – 943.
34. C. Meng, C. Liu, L. Chen, C. Hu and S. Fan, *Nano Lett.* 2010, **10**, 4025 – 4031.
35. A. Shanmugapriya, A. Srividhya, R. Ramya and P. N. Sudha, *Int. J. Environ. Sci.*, 2011, **1**, 2087 – 2095.
36. W. Zheng, B. Shen and W. Zhai, *New Progress on Graphene Research in Nanotechnology and Naomaterials*, Jian Ru Wong (Ed.) InTech, 2013.
<http://dx.doi.org/10.5772/50490>
37. X. Xia, W. Lei, Q. Hao, W. Wang and X. Wang, *Electrochim. Acta*, 2013, **99**, 253 – 261.
38. B. Shen, W. Zhai, C. Chen, D. Lu, J. Wang and W. Zheng, *Appl. Mater. And Interfaces*, 2011, **3**, 3103 – 3109.
39. X. Huang, X. Qi, F. Boey and H. Zhang, *Chem. Soc. Rev.* 2012, **41**, 666 – 686.
40. A. Shchukarev, B. Sundberg, E. Mellerowicz and P. Persson, *Surf. Interface Anal.*, 2002, **34**, 284 – 288.
41. R. Rozada, J. I. Paredes, S. V. Rodil, A. M. Alonso and J. M. D. Tascon, *Nano Res.* 2013, **6**, 216 – 233.
42. L. F. Wang, J. C. Duan, W. H. Miao, R. J. Zhang, S. Y. Pan and X. Y. Xu, *J. Hazardous Mater.*, 2011, **186**, 1681 – 1686.

43. H. J. Kwon, J. M. Ha, S. H. Yoo, G. Ali and S. O. Cho, *Nanoscale Res. Lett.*, 2014, **9**, 618/1 – 618/6.
44. J. G. Song, J. Park, W. Lee, T. Choi, H. Jung et al. *ACS Nano*, 2012, **7**, 11333 – 11340.
45. M. C. Liu, L. B. Kong, X. J. Ma, C. Lu, X. M. Li, Y. C. Luo and L. Kang, *New J. Chem.*, 2012, **36**, 1713 – 1716.
46. Z. Gao, W. Yang, J. Wang, B. Wang, Z. Li, Q. Liu, M. Zhang and L. Liu, *Energy & Fuels*, 2013, **27**, 568 – 575.
47. Z. Zhang, *Ultramicroscopy*, 2007, **107**, 598 – 603.
48. X. Xu, Z. Li, X. Tan, C. M. b. Holt, L. Zhang, B. S. Amirkhiz and D. Mitlin, *RSC Adv.*, 2012, **2**, 2753 – 2755.
49. L. Dambies, T. Vincent, A. Domard and E. Guibal, *Biomacromolecules*, 2001, **2**, 1198 – 1205.
50. G. K. Veerasubramani, K. Krishnamoorthy and S. J. Kim, *RSC Adv.*, 2015, **5**, 16319 – 16327.
51. C. Z. Yaun, X. G. Zhang, Q. F. Wu and B. Gao, *Solid State Ionics*, 2006, **177**, 1237 – 1242.
52. X. L. Huang, J. Chai, T. Jiang, Y. J. Wei, G. Chen, W. Q. Liu, D. Han, L. Niu, L. Wang and X.B. Zhang, *J. Mater. Chem. A*, 2012, **22**, 3404 – 3410.
53. X. Xu, J. Shen, N. Li and M. Ye, *J. Alloys and Compds.* 2014, **616**, 58 – 65.
54. B. Anothumakool, A. Torris, S. N. Bhange, S. M. Unni, M. V. Badiger and S. Kurungot, *Appl. Mater. Interfaces*, 2013, **5**, 13397 – 13404.
55. J. P. C. Trigueiro, R. S. Borges, R. L. Lavall, H. D. R. Calado and G. G. Silva, *Nano Res.*, 2009, **2**, 733 – 739.
56. X. Yu, B. Lu, and Z. Xu, *Adv. Mater.* 2014, **26**, 1044 – 1051.

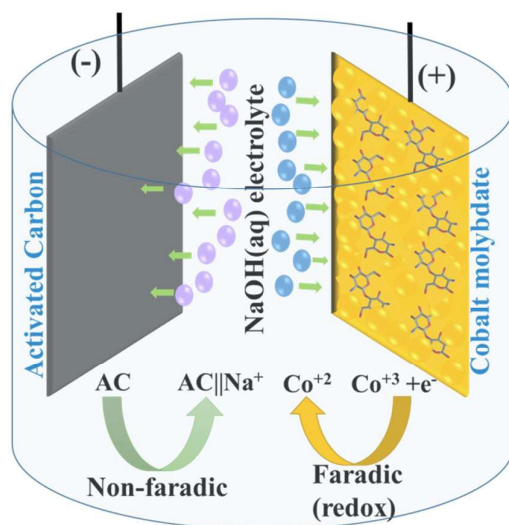
57. P. Staiti and F. Lufrano, *Electrochim. Acta*, 2010, **55**, 7436 - 7442.
58. M. Minakshi, D. Meyrick, and D. Appadoo, *Energy & Fuels*, 2013, **27**, 3516 – 3522.
59. X.-J. Ma, L.-B. Kong, W.-B. Zhang, M.-C. Liu, Y.-C. Luo, and L. Kang *Electrochim. Acta*, 2014, **130**, 660 – 669.

A biopolymer gel decorated cobalt molybdate nanowafer: Effective graft polymer cross-linked with an organic acid for better energy storage

Ramya Ramkumar and Manickam Minakshi Sundaram*

School of Engineering and Information Technology, Murdoch University, WA 6150, Australia

Table of Contents



Effective cross-linking strategy for grafting polymer with $CoMoO_4$ suits longevity for the fabricated hybrid energy storage device in aqueous solutions.